Tectonophysics, 47 (1978) 131—157

© Elsevier Scientific Publishing Company, Amsterdam — Printed in The Netherlands

OPHIOLITES, SEISMIC VELOCITIES AND OCEANIC CRUSTAL STRUCTURE

NIKOLAS I. CHRISTENSEN

Department of Geological Sciences and Graduate Program in Geophysics, University of Washington, Seattle, Wash. 98195 (U.S.A.)

(Received April 25, 1977; revised version accepted September 21, 1977)

ABSTRACT

Christensen, N.I., 1978. Ophiolites, seismic velocities and oceanic crustal structure. Tectonophysics, 47: 131—157.

Seismic velocities have been measured to pressures of 10 kbars for 96 cores of 36 rocks collected from ophiolite complexes. Average densities (ρ), compressional wave velocities (V_p), shear wave velocities (V_s) and Poisson's ratios (σ) at 1 kbar for major rock types are as follows:

Rock	ρ (g/cm^3)	V_p (km/sec)	V_s (km/sec)	σ
Serpentinite	2.53	5.05	2.45	0.35
Trondhjemite	2.69	6.33	3.67	0.25
Spilite	2.72	5.80	3.18	0.28
Metagabbro (greenschist facies)	2.81	6.52	3.62	0.28
Metagabbro (amphibolite facies)	2.99	6.95	3.73	0.29
Gabbro	3.00	7.20	3.80	0.31
Pyroxenite	3.24	7.82	4.25	0.29

Velocities in metagabbro and gabbro, the probable constituents of the lower oceanic crust, are highly dependent on mineralogy and mineral orientation. Both can be significantly anisotropic, the anisotropies originating from preferred hornblende orientation in metagabbro and olivine orientation in cumulate gabbro. Velocities in serpentinites depend upon amounts of relic olivine and pyroxene and serpentine mineralogy. Of significance, antigorite is faster than lizardite and chrysotile. Due primarily to a high quartz content, trondhjemite has a low Poisson's ratio. Velocity profiles constructed from reported petrology for the Vourinos, Troodos, Semail, Papua and Bay of Islands Massifs have much in common with seismic profiles of the oceanic crust. Major seismic discontinuities result from (1) increasing metamorphic grade with depth (the layer 2—3 boundary) and (2) a transition from gabbro, anorthosite and troctolite to dunite and peridotite (the Mohorovičić discontinuity).

Author's personal copy

INTRODUCTION

Oceanic crustal structure has been well defined by numerous seismic refraction studies and more recently by reflection profiling using multichan-

nel techniques. Of fundamental importance in interpreting seismic velocities in terms of petrology are laboratory investigations of elastic wave velocities in rocks. During the past few years the view that the ophiolite suite represents oceanic crust and upper mantle has gained considerable support and therefore it seems appropriate that a detailed study of velocities of different rock types from ophiolites be undertaken to test this hypothesis.

Velocities have been reported at elevated pressures for several rocks similar to those found in ophiolites. These include compressional wave velocities in basalt, diabase, quartz diorite, gabbro, anorthosite, dunite, serpentinite, amphibolite and greenstone (Birch, 1960; Christensen, 1965, 1966a, 1970; Manghnani and Woollard, 1968) and shear wave velocities in quartz diorite, gabbro, anorthosite, serpentinite and dunite (Simmons, 1964; Christensen, 1966a,b). More recently velocities have been reported for a variety of rocks dredged from the ocean floor (e.g., Christensen and Shaw, 1970; Barrett and Aumento, 1970; Fox et al., 1973; Christensen and Salisbury, 1975) and collected from several well known ophiolite localities (Poster, 1973, Peterson et al., 1974; Kroenke et al., 1976). To add to this large amount of data already available may seem unnecessary; however there is a need for more systematic sampling, especially of the metamorphic rocks common in many ophiolites. Also shear velocities and elastic parameters, such as Poisson's ratios which are particularly diagnostic of certain rock types (Christensen, 1972), are poorly known for many rocks common in ophiolites. Another important parameter, which greatly influences velocities in the pressure range of the oceanic crust, is water saturation (Nur and Simmons, 1969; Christensen and Salisbury, 1975). The earlier measurements cited above, including many of the velocities from ophiolites and dredged rocks, were not made on water saturated specimens, thereby creating some difficulty in using the data for the interpretation of oceanic refraction velocities in terms of petrology.

In this paper compressional and shear velocities are presented to hydrostatic confining pressures of 10 kbars for a variety of rock types collected from several ophiolite localities within the western United States. The samples have been water saturated prior to the runs, the directional dependence of velocity has been examined in detail and elastic constants have been calculated for each rock at several pressures. The velocity data are used to place the various rock types at appropriate levels within the oceanic crust and to construct detailed velocity profiles for several major ophiolite massifs.

EXPERIMENTAL DETAILS, SAMPLES AND NUMERICAL DATA

Velocities have been measured using the pulse transmission technique described in detail by Birch (1960). To investigate anisotropy, three cores, 2.54 cm in diameter and 5—8 cm in length, were cut with mutually perpendicular axes from most specimens. The reported densities are bulk densities calculated from the weights and dimensions of the cylindrical samples.

The sample, transducer and electrode assembly was similar to that

Author's personal copy

described by Birch (1960) and Simmons (1964). The transducers were 2.54 cm diameter barium titanate ceramic and AC-cut quartz crystals with 2 MHz natural resonant frequencies. Prior to the runs the samples were water saturated and 100 mesh screens were placed between the cores and copper jackets to provide space to allow water to drain from grain boundary cracks as confining pressure was increased. By this means, pore pressure was maintained much lower than confining pressure. The importance of water saturation and pore pressure on velocities in oceanic igneous and metamorphic rocks has been summarized by Christensen and Salisbury (1975). It has been demonstrated experimentally that water saturation significantly increases velocities at confining pressures less than approximately 1 kbar. High pore pressures, on the other hand, can lower velocities for a given confining pressure. These parameters are not believed to be significant at crustal depths below a few kilometers where fractures and grain boundary cracks have been sealed by metamorphic recrystallization and confining pressure.

The pressure system consisted of a two-stage intensifier using a low viscosity oil as the pressure medium. Pressure was measured by observing the change in electrical resistance of a calibrated manganin coil located on the high pressure side of the intensifier. The electronic components consisted of a pulse generator, a dual trace oscilloscope and a calibrated variable-length mercury delay line. The velocities are estimated to be accurate to one percent (Christensen and Shaw, 1970).

Several papers (e.g., Birch, 1960, Simmons, 1964) have discussed the differences in frequencies used in the laboratory and field refraction studies and have concluded that dispersion of seismic body waves in the frequency range of 10^{-1}—10^{7} cycles/sec is negligible. Thus the laboratory measurements may be directly applied to the interpretation of field measurements.

The rocks selected for this study were collected from several major ophiolite localities in the western United States (Fig. 1). Details of the structure and petrology of several of the California ophiolites are given by Lipman (1964), Bailey et al. (1970), Page (1972) and Goullaud (1975). The Canyon Mountain ophiolite has been studied by Thayer (1963) and Avé Lallemant (1976). Estimated modal mineralogy obtained from thin sections cut from core ends are given in Table I. Several samples are noteworthy because of the paucity of velocity data on these rock types: the trondhjemites are similar to the oceanic plagiogranites of Coleman and Peterman (1975); several metagabbros contain mineral assemblages characteristic of the prehnite—pumpellyite, greenschist and amphibolite facies; the spilites have mineralogies which are quite different from less altered basalts; two of the serpentinites differ significantly from previously studied serpentinites because they contain abundant antigorite.

Bulk densities (ρ), compressional wave velocities (V_p), shear wave velocities (V_s), the ratios of compressional to shear wave velocity (V_p/V_s), Poisson's ratios (σ), bulk moduli (K), shear moduli (μ), Lamé's constants (λ) and Young's moduli (E) are given in Table II at pressures to 10 kbar. Because of

Author's personal copy

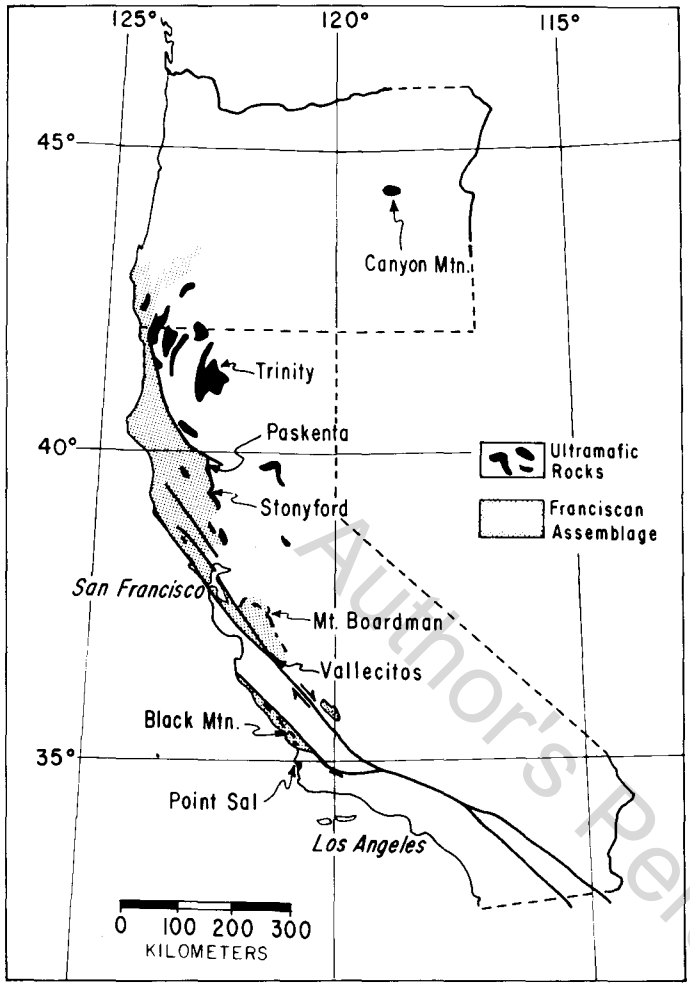

Fig. 1. Sample localities.

the relatively rapid increases in velocities over the first kilobar increase in pressure, which is attributed largely to grain boundary closure (Birch, 1961), velocities and elastic constants are given at smaller increments to 1 kbar. For samples of low anisotropy the data of Table II represent simple means of velocities measured in three directions and densities measured from three cores. This data is represented by a bar over the appropriate parameter. The elastic constants were calculated from the velocities and densities using the well known equations summarized by Birch (1961). Mean velocities and densities used in the calculations were corrected for dimension changes at high pressures using an iterative routine and the dynamically determined compressibilities. For the highly anisotropic specimens, compressional wave

Author's Personal Copy

TABLE I

Modal analyses * (Vol.%)

Sample	Plagioclase	Pyroxene	Amphibole	Olivine	Serpentine	Rest
Serpentinite Mt. Boardman, CA					95	5 op
Serpentinite Paskenta, CA					96	4 op
Serpentinite (1) Canyon Mtn, OR					95	5 op
Serpentinite (2) Canyon Mtn, OR					94	6 op Trace ch, sp, ta
Serpentinite (1) Black Mtn, CA		4 (opx)		3	90	3 op
Serpentinite (2) Black Mtn, CA		7 (opx)		trace	88	5 op Trace ch
Serpentinite (1) Stonyford, CA		20 (opx)		5	70	5 op
Trondhjemite (1) Trinity, CA	40 (sa)					40 qu, 17 ch, 3 op
Serpentinite (2) Stonyford, CA					95	5 op + ch Trace ca
Spilite (1) Black Mtn, CA	35 (al)					50 pu—ch—ep—sp, 15 ca
Spilite (2) Black Mtn, CA	45 (al)	15 (cpx)	trace			40 ch—ep—pu—sp
Spilite Canyon Mtn, CA	40 (al)	15 (cpx)	5			40 ca—ch—pu—sp—qu
P. Serp. peridotite Vallecitos, CA		5 (opx + cpx)		45	45	5 op
Metagabbro (1) Point Sal, CA	60 (al)		30			10 pr—pu—qu—sp
Trondhjemite (2) Trinity, CA	55 (sa)					44 qu, 5 ch, 1 sp
Spilite Mt. Boardman, CA	45 (al)					55 ch—ca—ep

Author's Personal Copy

TABLE I (*continued*)

Sample	Plagioclase	Pyroxene	Amphibole	Olivine	Serpentine	Rest
Metagabbro (1) Canyon Mtn, OR	30	2	18			50 pr—ca—ch
P. Serp. peridotite (1) Mt. Boardman, CA		23 (opx + cpx)	trace	65	10	2 op
Metagabbro (2) Point Sal, CA	50 (al)		40			8 qu, 2 op
Diabase Paskenta, CA	40 (al)	35 (cpx)				20 ch—ep—ca 5 sp
P. Serp. peridotite (2) Mt. Boardman, CA		23 (cpx + opx)	5	30	40	2 op
Metagabbro (2) Canyon Mtn, OR	50 (al)		40			5 sp, 1 ch, 4 pr
Metagabbro (1) Trinity, CA	40		35			23 ep, 2 sp
Amphibolite Canyon Mtn, OR	50		43			7 op—sp
Gabbro (1A) Canyon Mtn, OR	50	35 (cpx + opx)	5			10 pr
Gabbro (1B) Canyon Mtn, OR	50	40 (cpx + opx)	5	5	trace	

Author's Personal Copy

Gabbro (1C) Canyon Mtn, OR	40	40 (cpx + opx)	10	10	trace	
Gabbro (1D) Canyon Mtn, OR	40	20 (cpx)	5	15	20	
Metagabbro (3) Point Sal, CA	40 (sa)	25 (cpx)	35			
Metagabbro (2) Trinity, CA	35	10 (cpx)	50			4 qu, 1 sp
Gabbro (2) Canyon Mtn, OR	40 (sa)	35 (cpx + opx)	5		15	5 ch
Metagabbro (3) Trinity, CA	55 (sa)		40			2 op, 2 sp, 1 ch
Metagabbro (3) Canyon Mtn, OR	50 (sa)	15 (cpx)	25			5 ch, 2 sp, 3 op
Metagabbro (4) Trinity, CA	40 (sa)	trace	40			7 sp, 13 ch
Pyroxenite (1) Canyon Mtn, OR		90 (cpx + opx)	1	2	7	
Pyroxenite (2) Canyon Mtn, OR		84 (cpx + opx)		15	1	

* al = albite, ca = carbonate, ch = chlorite, cpx = clinopyroxene, ep = epidote, op = opaques, opx = orthopyroxene, pr = prehnite, pu = pumpellyite, qu = quartz, sp = sphene, sa = saussuritized plagioclase, ta = talc

Author's Personal Copy

TABLE II

Velocities, densities and elastic constants

P (kbar)	$\overline{V}_p$ (km/sec)	$\overline{V}_s$ (km/sec)	$\overline{V}_p/\overline{V}_s$	$\overline{\sigma}$	$\overline{K}$ (Mb)	$\overline{\mu}$ (Mb)	$\overline{\lambda}$ (Mb)	$\overline{E}$ (Mb)
Serpentinite, Mount Boardman, Calif. — $\overline{\rho}$ = 2.513 g/cm^3								
0.2	4.90	2.44	2.01	0.34	0.40	0.15	0.30	0.40
0.4	4.92	2.45	2.01	0.34	0.41	0.15	0.31	0.40
0.6	4.94	2.46	2.01	0.34	0.41	0.15	0.31	0.41
1.0	4.96	2.47	2.01	0.34	0.42	0.15	0.31	0.41
2.0	5.03	2.48	2.03	0.34	0.43	0.16	0.33	0.42
4.0	5.15	2.49	2.06	0.35	0.46	0.16	0.35	0.42
6.0	5.25	2.50	2.10	0.35	0.49	0.16	0.38	0.43
10.0	5.42	2.51	2.16	0.36	0.53	0.16	0.43	0.43
Serpentinite, Paskenta, Calif. — $\overline{\rho}$ = 2.517 g/cm^3								
0.2	4.89	2.40	2.04	0.34	0.41	0.15	0.31	0.39
0.4	4.93	2.42	2.04	0.34	0.42	0.15	0.32	0.39
0.6	4.96	2.43	2.04	0.34	0.42	0.15	0.32	0.40
1.0	5.00	2.44	2.04	0.34	0.43	0.15	0.33	0.40
2.0	5.07	2.46	2.06	0.35	0.44	0.15	0.34	0.41
4.0	5.19	2.50	2.08	0.35	0.47	0.16	0.36	0.43
6.0	5.31	2.54	2.09	0.35	0.50	0.16	0.39	0.44
10.0	5.49	2.57	2.14	0.36	0.54	0.17	0.43	0.46
Serpentinite (1), Canyon Mountain, Oreg. — $\overline{\rho}$ = 2.535 g/cm^3								
0.2	5.26	2.50	2.10	0.35	0.49	0.16	0.38	0.43
0.4	5.27	2.51	2.10	0.35	0.49	0.16	0.38	0.43
0.6	5.29	2.51	2.11	0.35	0.50	0.16	0.39	0.43
1.0	5.31	2.52	2.11	0.35	0.50	0.16	0.39	0.44
2.0	5.35	2.53	2.11	0.36	0.51	0.16	0.40	0.44
4.0	5.42	2.54	2.13	0.36	0.53	0.16	0.42	0.45
6.0	5.50	2.55	2.16	0.36	0.55	0.17	0.44	0.45
10.0	5.62	2.57	2.19	0.37	0.58	0.17	0.47	0.46
Serpentinite (2), Canyon Mountain, Oreg. — $\overline{\rho}$ = 2.550 g/cm^3								
0.2	4.78	2.36	2.03	0.34	0.39	0.14	0.30	0.38
0.4	4.82	2.38	2.03	0.34	0.40	0.14	0.30	0.39
0.6	4.85	2.39	2.03	0.34	0.41	0.15	0.31	0.39
1.0	4.90	2.40	2.04	0.34	0.42	0.15	0.32	0.39
2.0	4.99	2.43	2.05	0.34	0.43	0.15	0.33	0.41
4.0	5.11	2.46	2.08	0.35	0.46	0.15	0.36	0.42
6.0	5.21	2.48	2.10	0.35	0.49	0.16	0.38	0.43
10.0	5.38	2.52	2.18	0.36	0.52	0.16	0.42	0.44
Serpentinite (1), Black Mountain, Calif. — $\overline{\rho}$ = 2.623 g/cm^3								
0.2	5.51	2.66	2.07	0.35	0.55	0.19	0.43	0.50
0.4	5.52	2.67	2.07	0.35	0.55	0.19	0.43	0.50
0.6	5.54	2.67	2.07	0.35	0.56	0.19	0.43	0.50
1.0	5.56	2.68	2.07	0.35	0.56	0.19	0.44	0.51
2.0	5.63	2.70	2.09	0.35	0.58	0.19	0.45	0.52
4.0	5.71	2.71	2.11	0.36	0.60	0.19	0.47	0.52
6.0	5.78	2.72	2.12	0.36	0.62	0.19	0.49	0.53
10.0	5.89	2.73	2.16	0.36	0.65	0.20	0.52	0.54

Author's Personal Copy

TABLE II (*continued*)

P (kbar)	$\overline{V}_p$ (km/sec)	$\overline{V}_s$ (km/sec)	$\overline{V}_p/\overline{V}_s$	$\overline{\sigma}$	$\overline{K}$ (Mb)	$\overline{\mu}$ (Mb)	$\overline{\lambda}$ (Mb)	$\overline{E}$ (Mb)
Serpentine (2), Black Mountain, Calif. — $\overline{\rho}$ = 2.631 g/cm^3								
0.2	5.52	2.56	2.16	0.36	0.57	0.17	0.46	0.47
0.4	5.53	2.57	2.15	0.36	0.57	0.17	0.46	0.47
0.6	5.55	2.58	2.15	0.36	0.58	0.18	0.46	0.48
1.0	5.57	2.59	2.15	0.36	0.58	0.18	0.46	0.48
2.0	5.62	2.61	2.15	0.36	0.59	0.18	0.47	0.49
4.0	5.70	2.64	2.16	0.36	0.61	0.18	0.49	0.50
6.0	5.76	2.66	2.17	0.36	0.63	0.19	0.50	0.51
10.0	5.83	2.68	2.17	0.37	0.64	0.19	0.52	0.52
Serpentinite (1), Stonyford, Calif. — $\overline{\rho}$ = 2.632 g/cm^3								
0.2	5.76	2.80	2.06	0.35	0.60	0.21	0.46	0.56
0.4	5.83	2.84	2.06	0.35	0.61	0.21	0.47	0.57
0.6	5.87	2.87	2.05	0.34	0.62	0.22	0.47	0.58
1.0	5.92	2.92	2.03	0.34	0.62	0.22	0.47	0.60
2.0	6.00	3.03	1.98	0.33	0.63	0.24	0.46	0.64
4.0	6.10	3.16	1.95	0.32	0.63	0.26	0.45	0.69
6.0	6.18	3.19	1.94	0.32	0.65	0.27	0.47	0.71
10.0	6.31	3.24	1.95	0.32	0.68	0.28	0.50	0.73
Trondhjemite (1), Trinity Complex, Calif. — $\overline{\rho}$ = 2.648 g/cm^3								
0.2	6.00	3.56	1.69	0.23	0.51	0.34	0.28	0.82
0.4	6.12	3.58	1.71	0.24	0.54	0.34	0.31	0.84
0.6	6.20	3.60	1.72	0.25	0.56	0.34	0.33	0.86
1.0	6.28	3.63	1.73	0.25	0.58	0.35	0.35	0.87
2.0	6.37	3.66	1.74	0.25	0.60	0.36	0.37	0.89
4.0	6.48	3.72	1.74	0.25	0.62	0.37	0.38	0.92
6.0	6.56	3.75	1.75	0.26	0.65	0.37	0.40	0.94
10.0	6.71	3.81	1.76	0.26	0.68	0.39	0.43	0.98
Serpentinite (2), Stonyford, Calif. — $\overline{\rho}$ = 2.665 g/cm^3								
0.2	6.44	3.52	1.83	0.29	0.67	0.33	0.44	0.85
0.4	6.46	3.53	1.83	0.29	0.67	0.33	0.45	0.85
0.6	6.47	3.54	1.83	0.29	0.67	0.33	0.45	0.86
1.0	6.49	3.55	1.83	0.29	0.68	0.34	0.45	0.86
2.0	6.54	3.58	1.83	0.29	0.69	0.34	0.46	0.88
4.0	6.60	3.59	1.84	0.29	0.70	0.34	0.47	0.89
6.0	6.64	3.61	1.84	0.29	0.71	0.35	0.48	0.90
10.0	6.69	3.62	1.85	0.29	0.73	0.35	0.50	0.91
Spilite (1), Black Mountain, Calif. — $\overline{\rho}$ = 2.704 g/cm^3								
0.2	5.52	3.04	1.82	0.28	0.49	0.25	0.32	0.64
0.4	5.60	3.09	1.81	0.28	0.50	0.26	0.33	0.66
0.6	5.66	3.12	1.81	0.28	0.52	0.26	0.34	0.68
1.0	5.77	3.17	1.82	0.28	0.54	0.27	0.36	0.70
2.0	5.90	3.24	1.82	0.28	0.56	0.28	0.37	0.73
4.0	6.02	3.32	1.81	0.28	0.58	0.30	0.39	0.77
6.0	6.11	3.34	1.83	0.29	0.61	0.30	0.41	0.78
10.0	6.22	3.38	1.84	0.29	0.64	0.31	0.43	0.80

Author's personal copy

TABLE II (*continued*)

P (kbar)	$\overline{V}_p$ (km/sec)	$\overline{V}_s$ (km/sec)	$\overline{V}_p/\overline{V}_s$	$\overline{\sigma}$	$\overline{K}$ (Mb)	$\overline{\mu}$ (Mb)	$\overline{\lambda}$ (Mb)	$\overline{E}$ (Mb)
Spilite (2), Black Mountain, Calif. — $\overline{\rho}$ = 2.704 g/cm^3								
0.2	4.85	2.78	1.74	0.26	0.36	0.21	0.22	0.52
0.4	5.06	2.86	1.77	0.27	0.40	0.22	0.25	0.56
0.6	5.23	2.92	1.79	0.27	0.43	0.23	0.28	0.59
1.0	5.43	2.98	1.82	0.28	0.48	0.24	0.32	0.62
2.0	5.67	3.09	1.84	0.29	0.53	0.26	0.35	0.66
4.0	5.86	3.20	1.84	0.29	0.56	0.28	0.37	0.72
6.0	5.99	3.25	1.84	0.29	0.59	0.29	0.40	0.74
10.0	6.19	3.31	1.87	0.30	0.64	0.30	0.45	0.78
Spilite, Canyon Mountain, Calif. — $\overline{\rho}$ = 2.713 g/cm^3								
0.2	5.74	3.15	1.82	0.28	0.54	0.27	0.36	0.69
0.4	5.77	3.17	1.82	0.28	0.54	0.27	0.36	0.70
0.6	5.81	3.19	1.82	0.28	0.55	0.28	0.36	0.71
1.0	5.88	3.21	1.83	0.29	0.57	0.28	0.38	0.72
2.0	5.95	3.24	1.84	0.29	0.58	0.29	0.39	0.74
4.0	6.05	3.27	1.85	0.29	0.61	0.29	0.41	0.75
6.0	6.13	3.29	1.86	0.30	0.63	0.29	0.43	0.76
10.0	6.28	3.33	1.89	0.30	0.67	0.30	0.47	0.79

P (kbar)	V_{p1} (km/sec)	V_{p2} (km/sec)	V_{p3} (km/sec)	
Partially serpentinized peridotite, Vallecitos, Calif.				ρ_1 = 2.618 g/cm^3
0.2	6.00	6.08	6.57	ρ_2 = 2.709 g/cm^3
0.4	6.04	6.10	6.59	ρ_3 = 2.825 g/cm^3
0.6	6.05	6.11	6.60	
1.0	6.08	6.13	6.62	
2.0	6.14	6.18	6.67	
4.0	6.23	6.25	6.74	
6.0	6.29	6.30	6.80	
10.0	6.39	6.38	6.88	

P (kbar)	$\overline{V}_p$ (km/sec)	$\overline{V}_s$ (km/sec)	$\overline{V}_p/\overline{V}_s$	$\overline{\sigma}$	$\overline{K}$ (Mb)	$\overline{\mu}$ (Mb)	$\overline{\lambda}$ (Mb)	$\overline{E}$ (Mb)
Metagabbro (1), Point Sal, Calif. — ρ = 2.721 g/cm^3								
0.2	6.31	3.55	1.78	0.27	0.63	0.34	0.40	0.87
0.4	6.33	3.56	1.78	0.27	0.63	0.34	0.40	0.88
0.6	6.35	3.57	1.78	0.27	0.63	0.35	0.40	0.88
1.0	6.38	3.59	1.78	0.27	0.64	0.35	0.41	0.89
2.0	6.43	3.61	1.78	0.27	0.65	0.35	0.42	0.90
4.0	6.50	3.63	1.79	0.27	0.67	0.36	0.43	0.91
6.0	6.54	3.64	1.80	0.28	0.68	0.36	0.44	0.92
10.0	6.60	3.65	1.81	0.28	0.70	0.37	0.46	0.93
Trondhjemite (2), Trinity Complex, Calif. — $\overline{\rho}$ = 2.731 g/cm^3								
0.2	6.11	3.54	1.73	0.25	0.56	0.34	0.34	0.85
0.4	6.21	3.61	1.72	0.24	0.58	0.36	0.34	0.89
0.6	6.29	3.65	1.72	0.25	0.60	0.36	0.35	0.91

Author's Personal Copy

TABLE II (*continued*)

P (kbar)	$\overline{V}_p$ (km/sec)	$\overline{V}_s$ (km/sec)	$\overline{V}_p/\overline{V}_s$	$\overline{\sigma}$	$\overline{K}$ (Mb)	$\overline{\mu}$ (Mb)	$\overline{\lambda}$ (Mb)	$\overline{E}$ (Mb)
1.0	6.38	3.70	1.72	0.25	0.61	0.37	0.36	0.93
2.0	6.49	3.76	1.73	0.25	0.64	0.39	0.38	0.96
4.0	6.60	3.84	1.72	0.24	0.65	0.40	0.39	1.00
6.0	6.67	3.88	1.72	0.24	0.67	0.41	0.39	1.03
10.0	6.80	3.96	1.72	0.24	0.70	0.43	0.41	1.07
Spilite, Mount Boardman, Calif. — $\overline{\rho}$ = 2.738 g/cm^3								
0.2	5.66	3.22	1.76	0.26	0.50	0.28	0.31	0.72
0.4	5.72	3.34	1.71	0.24	0.49	0.31	0.28	0.76
0.6	5.77	3.37	1.71	0.24	0.50	0.31	0.29	0.77
1.0	5.87	3.40	1.73	0.25	0.52	0.32	0.31	0.79
2.0	6.03	3.46	1.74	0.25	0.56	0.33	0.34	0.82
4.0	6.14	3.53	1.74	0.25	0.58	0.34	0.35	0.86
6.0	6.20	3.55	1.75	0.26	0.59	0.35	0.36	0.87
10.0	6.28	3.58	1.76	0.26	0.62	0.35	0.38	0.89
Metagabbro (1), Canyon Mountain, Oreg. — $\overline{\rho}$ = 2.816 g/cm^3								
0.2	6.58	3.59	1.83	0.29	0.74	0.36	0.49	0.94
0.4	6.59	3.60	1.83	0.29	0.74	0.37	0.49	0.94
0.6	6.61	3.61	1.83	0.29	0.74	0.37	0.50	0.95
1.0	6.64	3.64	1.82	0.29	0.74	0.37	0.50	0.96
2.0	6.69	3.68	1.82	0.28	0.75	0.38	0.50	0.98
4.0	6.73	3.74	1.80	0.28	0.75	0.39	0.49	1.01
6.0	6.80	3.78	1.80	0.28	0.77	0.40	0.50	1.03
10.0	6.94	3.86	1.80	0.28	0.80	0.42	0.52	1.07
Partially serpentinized peridotite (1), Mount Boardman, Calif. — $\overline{\rho}$ = 2.836 g/cm^3								
0.2	6.07	3.28	1.85	0.29	0.64	0.31	0.43	0.79
0.4	6.09	3.29	1.85	0.29	0.64	0.31	0.44	0.79
0.6	6.11	3.30	1.85	0.29	0.65	0.31	0.44	0.80
1.0	6.14	3.31	1.86	0.30	0.66	0.31	0.46	0.80
2.0	6.19	3.32	1.87	0.30	0.67	0.31	0.47	0.82
4.0	6.26	3.34	1.87	0.30	0.69	0.32	0.48	0.83
6.0	6.31	3.35	1.88	0.30	0.71	0.32	0.49	0.83
10.0	6.38	3.36	1.90	0.31	0.73	0.32	0.52	0.84
Metagabbro (2), Point Sal, Calif. — ρ = 2.847 g/cm^3								
0.2	6.31	3.56	1.77	0.27	0.65	0.36	0.41	0.91
0.4	6.33	3.57	1.78	0.27	0.66	0.36	0.42	0.92
0.6	6.36	3.57	1.78	0.27	0.67	0.36	0.43	0.92
1.0	6.40	3.58	1.79	0.27	0.68	0.36	0.44	0.93
2.0	6.46	3.60	1.80	0.28	0.70	0.37	0.45	0.94
4.0	6.54	3.62	1.81	0.28	0.72	0.37	0.47	0.96
6.0	6.59	3.64	1.81	0.28	0.73	0.38	0.48	0.97
10.0	6.64	3.66	1.81	0.28	0.75	0.38	0.49	0.98
Diabase (altered), Paskenta, Calif, — ρ = 2.857 g/cm^3								
0.2	5.95	3.11	1.91	0.31	0.64	0.28	0.46	0.73
0.4	6.03	3.12	1.93	0.32	0.67	0.28	0.48	0.73
0.6	6.06	3.13	1.94	0.32	0.68	0.28	0.49	0.74

Author's personal copy

TABLE II (*continued*)

P (kbar)	$\bar{V}_p$ (km/sec)	$\bar{V}_s$ (km/sec)	$\bar{V}_p/\bar{V}_s$	$\bar{\sigma}$	$\bar{K}$ (Mb)	$\bar{\mu}$ (Mb)	$\bar{\lambda}$ (Mb)	$\bar{E}$ (Mb)
1.0	6.15	3.16	1.95	0.32	0.70	0.28	0.51	0.75
2.0	6.24	3.21	1.94	0.32	0.72	0.29	0.52	0.78
4.0	6.36	3.29	1.93	0.32	0.74	0.31	0.54	0.81
6.0	6.42	3.33	1.93	0.32	0.76	0.32	0.54	0.84
10.0	6.49	3.37	1.93	0.32	0.77	0.33	0.56	0.86
Partially serpentinized peridotite (2), Mount Boardman, Calif. — $\bar{\rho}$ = 2.866 g/cm^3								
0.2	6.10	3.25	1.88	0.30	0.66	0.30	0.46	0.79
0.4	6.14	3.27	1.88	0.30	0.67	0.31	0.47	0.80
0.6	6.21	3.28	1.89	0.31	0.69	0.31	0.49	0.81
1.0	6.24	3.29	1.89	0.31	0.70	0.31	0.49	0.81
2.0	6.29	3.32	1.90	0.31	0.71	0.32	0.50	0.83
4.0	6.37	3.34	1.91	0.31	0.74	0.32	0.52	0.84
6.0	6.43	3.36	1.91	0.31	0.75	0.32	0.54	0.85
10.0	6.51	3.38	1.93	0.32	0.78	0.33	0.56	0.86
Metagabbro (2), Canyon Mountain, Oreg. — $\bar{\rho}$ = 2.871 g/cm^3								
0.2	6.61	3.64	1.82	0.28	0.75	0.38	0.49	0.98
0.4	6.63	3.64	1.82	0.28	0.75	0.38	0.50	0.98
0.6	6.64	3.65	1.82	0.28	0.76	0.38	0.50	0.98
1.0	6.66	3.66	1.82	0.28	0.76	0.38	0.50	0.99
2.0	6.70	3.68	1.82	0.28	0.77	0.39	0.51	1.00
4.0	6.75	3.70	1.82	0.28	0.79	0.39	0.52	1.01
6.0	6.78	3.72	1.82	0.28	0.79	0.40	0.53	1.02
10.0	6.84	3.76	1.82	0.28	0.81	0.41	0.53	1.04
Metagabbro (1), Trinity Complex, Calif. — $\bar{\rho}$ = 2.907 g/cm^3								
0.2	6.83	3.54	1.93	0.32	0.87	0.36	0.63	0.96
0.4	6.84	3.56	1.92	0.32	0.87	0.37	0.63	0.97
0.6	6.86	3.57	1.92	0.31	0.87	0.37	0.63	0.97
1.0	6.88	3.60	1.91	0.31	0.87	0.38	0.62	0.99
2.0	6.93	3.65	1.90	0.31	0.88	0.39	0.62	1.01
4.0	7.01	3.71	1.89	0.31	0.90	0.40	0.63	1.05
6.0	7.07	3.75	1.89	0.30	0.91	0.41	0.64	1.07
10.0	7.17	3.81	1.88	0.30	0.93	0.42	0.65	1.10

P (kbar)	V_{p1} (km/sec)	V_{p2} (km/sec)	V_{p3} (km/sec)	
Amphibolite, Canyon Mountain, Oreg.				ρ_1 = 2.914 g/cm^3
0.2	6.34	6.59	6.98	ρ_2 = 2.915 g/cm^3
0.4	6.36	6.61	6.99	ρ_3 = 2.947 g/cm^3
0.6	6.38	6.63	7.01	
1.0	6.40	6.66	7.03	
2.0	6.45	6.71	7.07	
4.0	6.51	6.78	7.11	
6.0	6.54	6.81	7.13	
10.0	6.57	6.84	7.16	

Author's Personal Copy

TABLE II (*continued*)

P (kbar)	V_{p1} (km/sec)	V_{p2} (km/sec)	V_{p3} (km/sec)	
Gabbro (1A), Canyon Mountain, Oreg.				ρ_1 = 2.918 g/cm^3
0.2	6.83	6.97	6.65	ρ_2 = 2.887 g/cm^3
0.4	6.86	6.99	6.70	ρ_3 = 2.887 g/cm^3
0.6	6.89	7.02	6.76	
1.0	6.92	7.06	6.80	
2.0	6.98	7.11	6.95	
4.0	7.07	7.19	7.13	
6.0	7.14	7.26	7.18	
10.0	7.24	7.38	7.28	
Gabbro (1B) Canyon Mountain, Oreg.				ρ_1 = 2.988 g/cm^3
0.2	7.13	7.18	7.17	ρ_2 = 2.985 g/cm^3
0.4	7.15	7.20	7.20	ρ_3 = 2.989 g/cm^3
0.6	7.17	7.21	7.23	
1.0	7.21	7.23	7.27	
2.0	7.27	7.27	7.32	
4.0	7.35	7.33	7.37	
6.0	7.43	7.38	7.42	
10.0	7.53	7.50	7.48	
Gabbro (1C), Canyon Mountain, Oreg.				ρ_1 = 2.987 g/cm^3
0.2	7.16	7.29	6.95	ρ_2 = 2.994 g/cm^3
0.4	7.19	7.31	6.98	ρ_3 = 2.980 g/cm^3
0.6	7.22	7.32	7.01	
1.0	7.25	7.34	7.05	
2.0	7.32	7.37	7.13	
4.0	7.39	7.42	7.23	
6.0	7.43	7.47	7.32	
10.0	7.52	7.57	7.42	
Gabbro (1D), Canyon Mountain, Oreg.				ρ_1 = 2.841 g/cm^3
0.2	6.63	6.72	6.32	ρ_2 = 2.841 g/cm^3
0.4	6.66	6.75	6.36	ρ_3 = 2.835 g/cm^3
0.6	6.68	6.78	6.39	
1.0	6.71	6.81	6.43	
2.0	6.76	6.86	6.51	
4.0	6.84	6.94	6.58	
6.0	6.92	7.02	6.62	
10.0	7.03	7.13	6.70	

Author's Personal Copy

TABLE II (*continued*)

P (kbar)	$\overline{V}_p$ (km/sec)	$\overline{V}_s$ (km/sec)	$\overline{V}_p/\overline{V}_s$	$\overline{\sigma}$	$\overline{K}$ (Mb)	$\overline{\mu}$ (Mb)	$\overline{\lambda}$ (Mb)	$\overline{E}$ (Mb)
Metagabbro (3), Point Sal, Calif. — ρ = 2.936 g/cm^3								
0.2	6.94	3.64	1.91	0.31	0.90	0.39	0.64	1.02
0.4	7.01	3.66	1.92	0.31	0.92	0.39	0.66	1.03
0.6	7.06	3.68	1.92	0.31	0.93	0.40	0.67	1.04
1.0	7.13	3.71	1.92	0.31	0.96	0.40	0.69	1.06
2.0	7.23	3.78	1.91	0.31	0.98	0.42	0.70	1.10
4.0	7.30	3.89	1.88	0.30	0.98	0.44	0.68	1.16
6.0	7.35	3.96	1.86	0.30	0.98	0.46	0.67	1.19
10.0	7.39	3.99	1.85	0.29	0.98	0.47	0.67	1.22

P (kbar)	V_{p1} (km/sec)	V_{p2} (km/sec)	
Metagabbro (2), Trinity Complex, Calif.			
0.2	7.08	7.21	ρ_1 = 2.918 g/cm^3
0.4	7.10	7.25	ρ_2 = 3.070 g/cm^3
0.6	7.12	7.29	
1.0	7.15	7.34	
2.0	7.20	7.42	
4.0	7.29	7.51	
6.0	7.34	7.58	
10.0	7.42	7.70	

P (kbar)	$\overline{V}_p$ (km/sec)	$\overline{V}_s$ (km/sec)	$\overline{V}_p/\overline{V}_s$	$\overline{\sigma}$	$\overline{K}$ (Mb)	$\overline{\mu}$ (Mb)	$\overline{\lambda}$ (Mb)	$\overline{E}$ (Mb)
Gabbro (2), Canyon Mountain, Oreg. — $\overline{\rho}$ = 3.013 g/cm^3								
0.2	6.84	3.67	1.86	0.30	0.87	0.41	0.60	1.05
0.4	6.88	3.69	1.86	0.30	0.88	0.41	0.61	1.07
0.6	6.91	3.72	1.86	0.30	0.88	0.42	0.61	1.08
1.0	6.97	3.76	1.85	0.29	0.90	0.43	0.61	1.10
2.0	7.07	3.82	1.85	0.29	0.92	0.44	0.63	1.14
4.0	7.18	3.90	1.84	0.29	0.94	0.46	0.64	1.18
6.0	7.26	3.94	1.84	0.29	0.97	0.47	0.65	1.21
10.0	7.40	4.02	1.84	0.29	1.00	0.49	0.68	1.26
Metagabbro (3), Trinity Complex, Calif. — $\overline{\rho}$ = 3.016 g/cm^3								
0.2	6.76	3.74	1.81	0.28	0.82	0.42	0.53	1.08
0.4	6.78	3.76	1.81	0.28	0.82	0.43	0.54	1.09
0.6	6.80	3.76	1.81	0.28	0.83	0.43	0.54	1.09
1.0	6.83	3.78	1.81	0.28	0.83	0.43	0.54	1.10
2.0	6.88	3.81	1.81	0.28	0.85	0.44	0.55	1.12
4.0	6.96	3.85	1.81	0.28	0.86	0.45	0.57	1.15
6.0	7.01	3.87	1.81	0.28	0.88	0.45	0.58	1.16
10.0	7.09	3.89	1.82	0.28	0.91	0.46	0.61	1.18

Author's Personal Copy

TABLE II (*continued*)

P (kbar)	$\overline{V}_p$ (km/sec)	$\overline{V}_s$ (km/sec)	$\overline{V}_p/\overline{V}_s$	$\overline{\sigma}$	$\overline{K}$ (Mb)	$\overline{\mu}$ (Mb)	$\overline{\lambda}$ (Mb)	$\overline{E}$ (Mb)
Metagabbro (3), Canyon Mountain, Oreg. — $\overline{\rho}$ = 3.034 g/cm^3								
0.2	6.92	3.74	1.85	0.29	0.89	0.42	0.60	1.10
0.4	6.96	3.75	1.86	0.30	0.90	0.43	0.62	1.11
0.6	6.99	3.77	1.85	0.29	0.91	0.47	0.62	1.12
1.0	7.03	3.79	1.85	0.30	0.92	0.44	0.63	1.13
2.0	7.10	3.83	1.85	0.29	0.94	0.45	0.64	1.15
4.0	7.18	3.89	1.85	0.29	0.95	0.46	0.65	1.19
6.0	7.23	3.93	1.84	0.29	0.96	0.47	0.65	1.21
10.0	7.33	4.01	1.83	0.29	0.98	0.49	0.66	1.26
Metagabbro (4), Trinity Complex, Calif. — $\overline{\rho}$ = 3.038 g/cm^3								
0.2	6.82	3.71	1.84	0.29	0.86	0.42	0.58	1.08
0.4	6.84	3.71	1.84	0.29	0.86	0.42	0.59	1.08
0.6	6.86	3.73	1.84	0.29	0.87	0.42	0.58	1.09
1.0	6.88	3.75	1.83	0.29	0.87	0.43	0.58	1.10
2.0	6.93	3.79	1.83	0.29	0.88	0.44	0.59	1.12
4.0	6.99	3.83	1.83	0.29	0.89	0.45	0.59	1.15
6.0	7.04	3.85	1.83	0.29	0.91	0.45	0.61	1.16
10.0	7.12	3.87	1.84	0.29	0.94	0.46	0.63	1.18
Pyroxenite (1), Canyon Mountain, Oreg. — $\overline{\rho}$ = 3.209 g/cm^3								
0.2	7.73	4.22	1.83	0.29	1.15	0.57	0.77	1.47
0.4	7.75	4.23	1.83	0.29	1.16	0.57	0.78	1.48
0.6	7.78	4.24	1.83	0.29	1.17	0.58	0.79	1.49
1.0	7.81	4.26	1.83	0.29	1.18	0.58	0.79	1.50
2.0	7.86	4.29	1.83	0.29	1.20	0.59	0.80	1.52
4.0	7.91	4.33	1.83	0.29	1.21	0.60	0.81	1.55
6.0	7.95	4.35	1.83	0.29	1.22	0.61	0.82	1.56
10.0	8.03	4.39	1.83	0.29	1.25	0.62	0.83	1.60
Pyroxenite (2), Canyon Mountain, Oreg. — $\overline{\rho}$ = 3.267 g/cm^3								
0.2	7.74	4.16	1.86	0.30	1.20	0.57	0.83	1.47
0.4	7.77	4.18	1.86	0.30	1.21	0.57	0.83	1.48
0.6	7.80	4.20	1.86	0.30	1.21	0.58	0.84	1.49
1.0	7.83	4.23	1.85	0.29	1.22	0.58	0.83	1.51
2.0	7.89	4.26	1.85	0.29	1.24	0.59	0.85	1.54
4.0	7.96	4.30	1.85	0.29	1.27	0.60	0.86	1.56
6.0	8.00	4.31	1.86	0.30	1.28	0.61	0.88	1.57
10.0	8.08	4.33	1.87	0.30	1.32	0.61	0.91	1.59

velocities are reported for three directions. Shear velocities were not measured for these specimens because of the dependence of shear velocity on displacement as well as propagation direction (Christensen, 1966b).

OPHIOLITE SEISMIC PROPERTIES AND MINERALOGY

In addition to mineralogy, a major factor influencing velocities of the upper oceanic crust is fracturing. The depth to which fracturing is important

Author's Personal Copy

is presently unknown, however sonobuoy data and results from the Deep Sea Drilling Project indicate that shattered and fractured volcanic material is common in the upper half kilometer of layer 2 (Hyndman and Drury, 1976). At greater depths elevated temperatures and pressures and associated metamorphism have likely healed most fractures (Christensen and Salisbury, 1975) and seismic velocities provide significant information on crustal mineralogy. In the following discussion mineralogy is correlated with velocities and elastic properties at 1 kbar, a pressure appropriate for the upper portion of oceanic layer 3.

Serpentinites

The first detailed study of compressional wave velocities in serpentinites at elevated pressures was that of Birch (1960, 1961), which demonstrated that compressional wave velocities increase with increasing density of serpentinites, the increase being related to relic olivine and pyroxene. Compressional wave velocities in partially serpentinized dunites and peridotites were found to possess an additional complexity, seismic anisotropy originating from preferred mineral orientation. Christensen (1966a) reported the elastic properties for a suite of ultramafics with variable serpentinization, which provided velocity—density curves for shear as well as compressional wave velocities. Of particular significance was the finding that serpentinite has a relatively high Poisson's ratio, an elastic parameter important in estimating crustal composition from seismic velocities.

Ranges of elastic properties and densities of the major rock types are summarized in Table III. Rock types for which single samples were studied are not included in the summary. Comparisons of the serpentinite data with that of the other rocks illustrate the high Poisson's ratios and relatively low velocities and elastic constants of serpentinites from ophiolites. The serpentinites with densities below 2.60 g/cm^3 are relatively pure, containing primarily a mixture of lizardite and chrysotile, and uniform in velocities and elastic constants. Elastic properties of serpentinites with densities between 2.60 and 2.70 g/cm^3 are, on the other hand, quite variable. This is partially due to accessory pyroxene and olivine and, more importantly, significant amounts of antigorite within the two serpentinites from Stonyford, California. A comparison of the elastic properties of serpentinite (2) from Stonyford, with other serpentinites (Table II) illustrates the relatively high velocities, low σ and high K, μ and E of antigorite. Thus velocities and elastic constants of serpentinites are strongly influenced by serpentine mineralogy as well as accessory mineralogy.

Spilites

Compared with serpentinites, the spilites have fairly narrow ranges in velocities, densities and elastic constants. Since spilite velocities are much

Author's personal copy

lower than velocities in fresh oceanic basalts ($V_p \simeq 6.5$ km/sec, $V_s \simeq 3.4$ km/sec; Christensen and Salisbury, 1975), spilitization is a significant process affecting elastic properties. The spilite with the lowest velocities, spilite 2 from Black Mountain, California, differs from the other three spilites in its lack of abundant groundmass calcite. Calcite is a relatively fast mineral (Birch, 1961) and is apparently responsible for the higher velocities and values of K, μ, λ and E in the Black Mountain (1), Canyon Mountain and Mount Boardman spilites. The Mount Boardman spilite differs from the other spilites because of its relatively low Poisson's ratio (0.25 at 1 kbar), which is attributed to a high quartz content. Since quartz has an extremely low Poisson's ratio (0.09; Birch, 1961) compared with common rock forming minerals, significant amounts of quartz in a rock have a profound influence on lowering Poisson's ratio.

Trondhjemites

The two trondhjemites included in this study have similar velocities and elastic constants. Even though their densities are similar to spilites, trondhjemite velocites are over 10% higher. Also their compressional wave velocities and values of K, λ and E are lower than similar properties of the metagabbros and gabbros (Table II). Shear velocities, on the other hand, and corresponding values of shear moduli are relatively high, producing low (0.25) Poisson's ratios. As with the Mount Boardman spilite, the high shear velocities and low Poisson's ratios are a consequence of abundant quartz.

Metagabbros

The metagabbros show wide ranges of densities, velocities and elastic constants. The lower density rocks (<2.90 g/cm^3) contain mineral assemblages characteristic of the prehnite—pumpellyite and greenschist facies. For these samples the plagioclase is highly albitized. Two samples (metagabbros (1) and (2), Point Sal, Calif.) contain abundant quartz and thus have relatively low Poisson's ratios (0.27). The intermediate density metagabbros (2.9—3.0 g/cm^3) contain saussuritized plagioclase with green hornblende and actinolite. They have relatively high compressional wave velocities (6.88—7.13 km/sec) and Poisson's ratios (0.31). The highest density metagabbros (>3.0 g/cm^3) contain amphibolite facies mineral assemblages, sometimes with overprints of the greenschist facies. Poisson's ratios vary from 0.28 to 0.30 and compressional wave velocities at 1 kbar range from 6.83 to 7.03 km/sec.

The amphibolite from Canyon Mountain is strongly foliated due to preferred hornblende orientation, which produces the high anisotropy (6.40—7.03 km/sec at 1 kbar). The fast direction corresponds to propagation parallel to a maximum concentration of hornblende c-axes (Christensen, 1965).

Author's Personal Copy

TABLE III

Properties at 1 kbar

	Number of samples	ρ (g/cm^3	V_p (km/sec)	V_s (km/sec)	σ	K (Mb)	μ (Mb)	λ (Mb)	E (Mb)
Serpentinites ($\rho < 2.60$ g/cm^3)	4	2.51—2.55	4.90—5.31	2.40—2.52	0.34—0.35	0.42—0.50	0.15—0.16	0.31—0.39	0.39—0.44
Serpentinites ($\rho > 2.60$ g/cm^3)	4	2.62—2.66	5.56—6.49	2.59—3.55	0.29—0.36	0.56—0.58	0.18—0.34	0.44—0.47	0.48—0.86
Spilites	4	2.70—2.74	5.43—5.88	2.98—3.40	0.25—0.29	0.48—0.57	0.24—0.32	0.31—0.38	0.62—0.79
Trondhjemites	2	2.65—2.73	6.28—6.38	3.63—3.70	0.25	0.58—0.61	0.35—0.39	0.35—0.36	0.87—0.93
Metagabbros	9	2.72—3.04	6.38—7.13	3.58—3.79	0.27—0.31	0.64—0.96	0.35—0.44	0.41—0.69	0.89—1.13
Gabbros	5 *	2.84—3.01	6.43—7.34	3.76	0.29	0.90	0.43	0.61	1.10
Pyroxenites	2	3.21—3.27	7.81—7.83	4.23—4.26	0.29	1.18—1.22	0.56	0.79—0.83	1.50—1.51
Partially serpentinized peridotite	3	2.62—2.87	6.08—6.62	3.29—3.31	0.30—0.31	0.66—0.70	0.31	0.44—0.49	0.80—0.81

* V_p only for four samples.

Author's Personal Copy

Gabbros

A large number of velocity measurements have been reported for gabbros (e.g., Birch, 1960; Simmons, 1964; Christensen, 1965; Fox et al., 1973; Kroenke et al., 1976). Compressional and shear velocities in relatively unaltered dredge samples range from 6.9 to 7.2 km/sec and 3.6 to 3.9 km/sec, respectively, whereas Poisson's ratios are generally between 0.29 and 0.31 (Christensen and Salisbury, 1975). Higher velocities are possible in olivine rich gabbros (Christensen, 1965).

A large block of cumulate gabbro (Canyon Mountain 1) was collected for a detailed anisotropy study (Fig. 2). Cores were removed from four levels (A, B, C and D, Table II) of one cumulate layer. At each level velocities were measured in three perpendicular directions, two parallel and one normal to the layering. Mineralogies of each level are given in Table I and velocities are summarized in Fig. 2.

Preferred orientations of plagioclase and pyroxene in the upper levels (A and B) of the gabbro are weak, thus these levels are nearly isotropic. Levels C and D, however, contain abundant olivine with a strong preferred orientation (Fig. 3), such that olivine *b* crystallographic axes form a maximum nearly normal to the cumulate layering, and the *a*- and *c*-axes tend to form partial girdles with well defined maxima within the layering. This is a common type of olivine orientation (Brothers, 1959), which produces seismic anisotropy with a slow velocity parallel to the olivine *b*-axes maxima (Christensen, 1966a). The increase in velocity going downward from levels

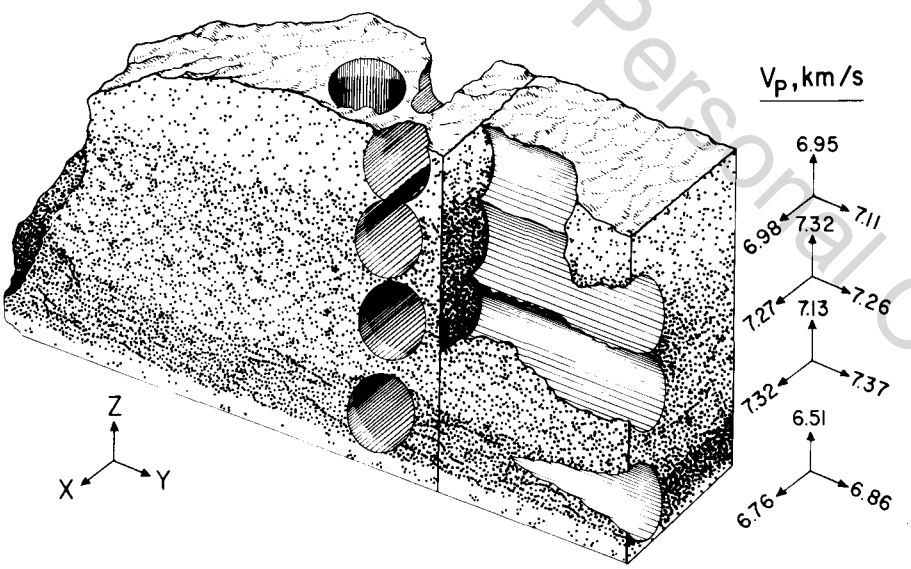

Fig. 2. Cumulate gabbro (Canyon Mountain 1) showing orientations of cores and compressional wave velocities at 2 kbar.

Rights Personal Copy

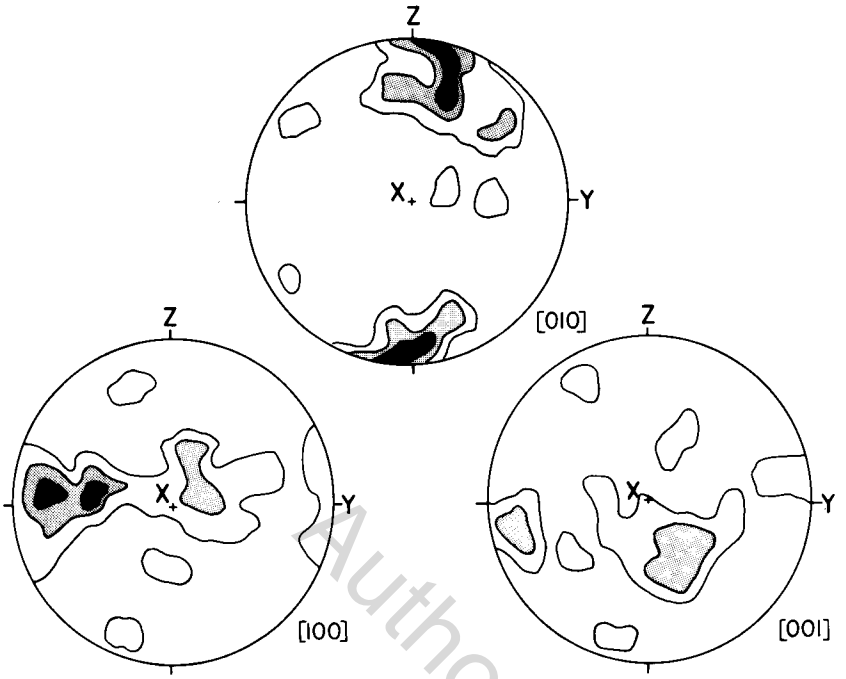

Fig. 3. Olivine orientation at levels C and D in Gabbro 1 from Canyon Mountain Contours 5, 3 and 1% per 1% area.

A to C is due to the increasing percentages of mafic minerals (Table I). The lower velocities of level D are a consequence of serpentinization.

Pyroxenities

The velocities of the two pyroxenites included in this study compare favorably with those reported by Birch (1960) for a pyroxenite from Sonoma County, Calif. The higher density pyroxenite has less serpentine and more accessory olivine. Although clinopyroxene is present in both rocks, they primarily contain enstatite.

DETAILED SEISMIC STRUCTURE OF OPHIOLITES

Several studies of compressional wave velocities have demonstrated that many rocks of the ophiolite suite have velocities similar to oceanic crustal refraction velocities (e.g., Birch, 1960: Poster, 1973; Peterson et al., 1974; Christensen and Salisbury, 1975; Hyndman and Drury, 1976). A similar correlation is illustrated in Fig. 4 for the rocks included in Table II. Superimposed in Fig. 4, in which observed velocities from 415 main ocean basin sites are presented in histogram form (Christensen and Salisbury, 1975), are

Author's Personal Copy

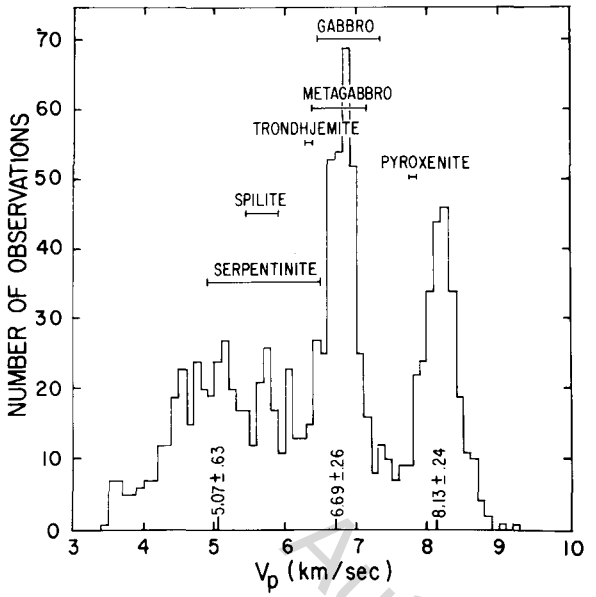

Fig. 4. Histogram of compressional wave refraction velocities from 415 main ocean basin sites (Christensen and Salisbury, 1975). Superimposed are ranges of velocities for the major rock types included in this study.

Author's Personal Copy

mean compressional wave velocities and standard deviations of velocity for layer 2, layer 3 and the upper mantle computed by Raitt (1963).

The similarities of gabbro and metagabbro velocities to lower oceanic crustal velocities are striking. Compressional wave velocities in serpentinites, partially serpentinized peridotites and trondhjemites, on the other hand, are lower than average layer 3 velocities. Velocities of the spilites are in the range of many layer 2 velocities. The pyroxenite velocities fall between Raitt's average 6.69 and 8.13 km/sec velocities, suggesting that pyroxenites are not major constituents of either the lower oceanic crust or the upper mantle.

The ophiolite bodies from which samples of the present study were collected are structurally complicated due to faulting which has dispersed critical stratigraphic levels (Bailey et al., 1970). Thus it is impossible to reconstruct detailed stratigraphic columns for these ophiolites so velocity profiles can be estimated for comparisons with oceanic crustal seismic refraction structure. Several ophiolite complexes, however, appear to be complete or nearly complete over large areas (e.g., Wilson, 1959; Smith, 1958; Moores, 1969; Davies, 1971; Williams, 1971; Reinhardt, 1969) and from the petrologic descriptions presented for these complexes and the data of Table II it is possible to estimate their detailed velocity structure.

Stratigraphic columns summarized by Christensen and Salisbury (1975) for the Vourinos complex of northern Greece, the Troodos complex of

Cyprus, the Semail complex of Oman, Papua of New Guinea and the Bay of Islands complex of Newfoundland are shown in Figs. 5 and 6, with estimated compressional (V_p) and shear (V_s) velocity profiles. The velocity profiles have been determined primarily from the data of Tables I and II, although the data of Hamilton et al. (1974), Birch (1960), Christensen (1966a) and Christensen and Salisbury (1972) have been used for sediment, basalt, anorthosite and peridotite velocities. The new data presented in this paper have been particularly useful in constructing the shear velocity columns and incorporating the influence of metamorphic grade on the velocity columns. It should be emphasized that since these complexes are currently under investigation, their columns are subject to revision (Christensen and Salisbury, 1975).

Average upper crustal layer 2 seismic refraction velocities are likely influenced by extensive low temperature weathering in regions of old oceanic crust (Christensen and Salisbury, 1972) and large scale fracturing (Hyndman and Drury, 1976). Submarine weathering has been observed to decrease velocities as much as 40% (Christensen and Salisbury, 1975), whereas fracturing, possibly in conjunction with intercalated sediments, has been estimated to locally lower layer 2 velocities as high as 70% (Hyndman and Drury, 1976). In Figs. 5 and 6 velocities in the uppermost levels of the

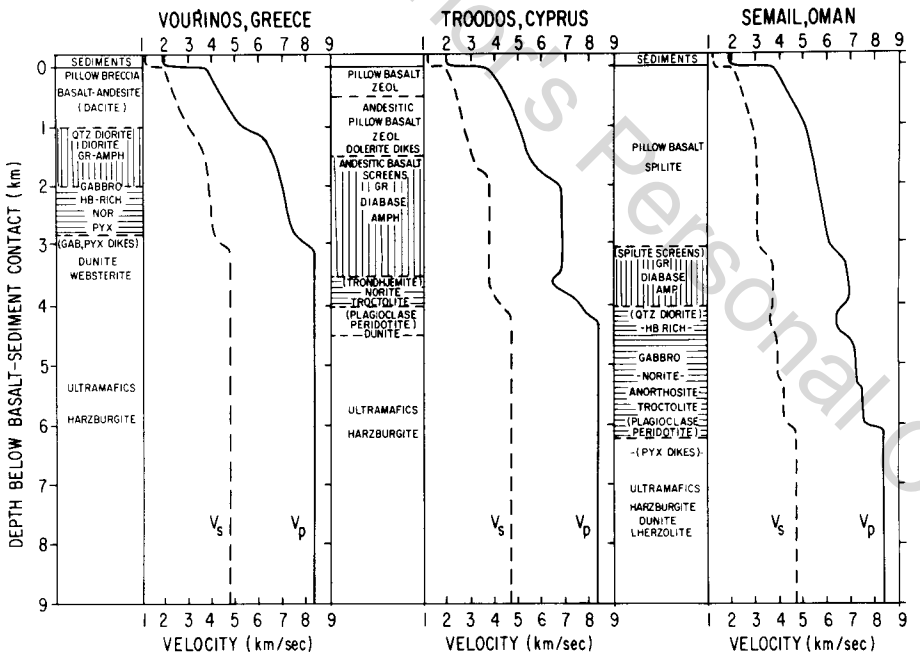

Fig. 5. Stratigraphic columns and estimated velocities in major ophiolite complexes (see text). Metamorphic facies: *zeol* = zeolite, *pre-pump* = prehnite-pumpellyite, *gr* = greenschist, *amp* = amphibolite. Vertical and horizontal striping represents sheeted dikes and cumulate layering, respectively.

Author's Personal Copy

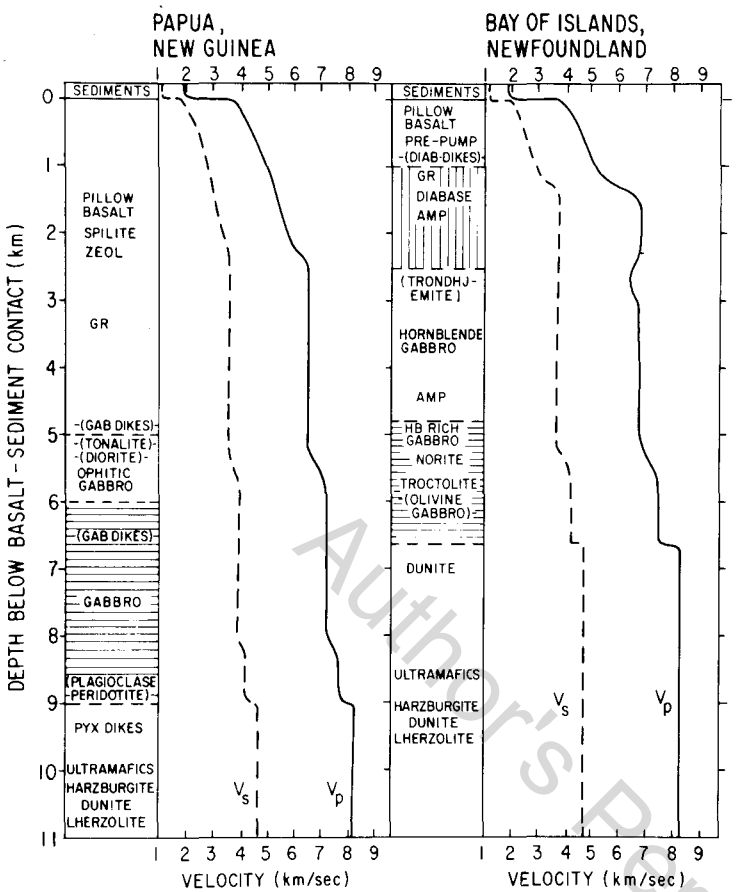

Fig. 6. Stratigraphic columns and estimated velocities (abbreviations similar to Fig. 5).

Author's Personal Copy

pillow basalt sections of each complex have been lowered to 40% of measured velocities in relatively fresh basalts. It has been assumed that the influences of fracturing and weathering diminish with depth, so velocities at 1 km below the basalt—sediment interface are related primarily to mineralogy.

Neglecting the obvious sharp increase in velocities at the bases of the sedimentary sections, the first major seismic discontinuities occur at approximately 1 km depths in the Vourinos and Bay of Islands complexes, 1.5 km in Troodos, 2 km in Papua and 3 km in the Semail complex. These regions of rapid increases in velocities are related to increasing metamorphic grade and are interpreted as being capable of producing a seismic discontinuity similar to the layer 2—3 seismic boundary of refraction seismology.

A second major seismic discontinuity predicted in all of the complexes is associated with the change from gabbro, anorthosite and troctolite to

dunite and peridotite. This corresponds to the crust—mantle boundary in which compressional wave velocities generally increase to over 8 km/sec. Variations in upper mantle velocities would depend on many factors, the more important being accessory mineralogy, anisotropy due to preferred mineral orientation and the temperature regime of the upper mantle. Other seismic discontinuities likely to occur within the crustal sections are related to (1) the transition from relatively olivine free gabbro to olivine gabbro, anorthosite and troctolite (Semail and Bay of Islands) and (2) the transition of greenschist facies metamorphics and tonalite to gabbro (Papua).

Three of the sections (Troodos, Semail and Bay of Islands) have regions with distinct compressional wave velocity inversions associated with late differentiates, such as trondhjemite and quartz diorite. It is significant that these inversions occur only when amphibolite facies rocks are above the late differentiates (Figs. 5 and 6). Also, shear velocity inversions are nonexistent or minimal since the late differentiates have relatively low Poisson's ratios

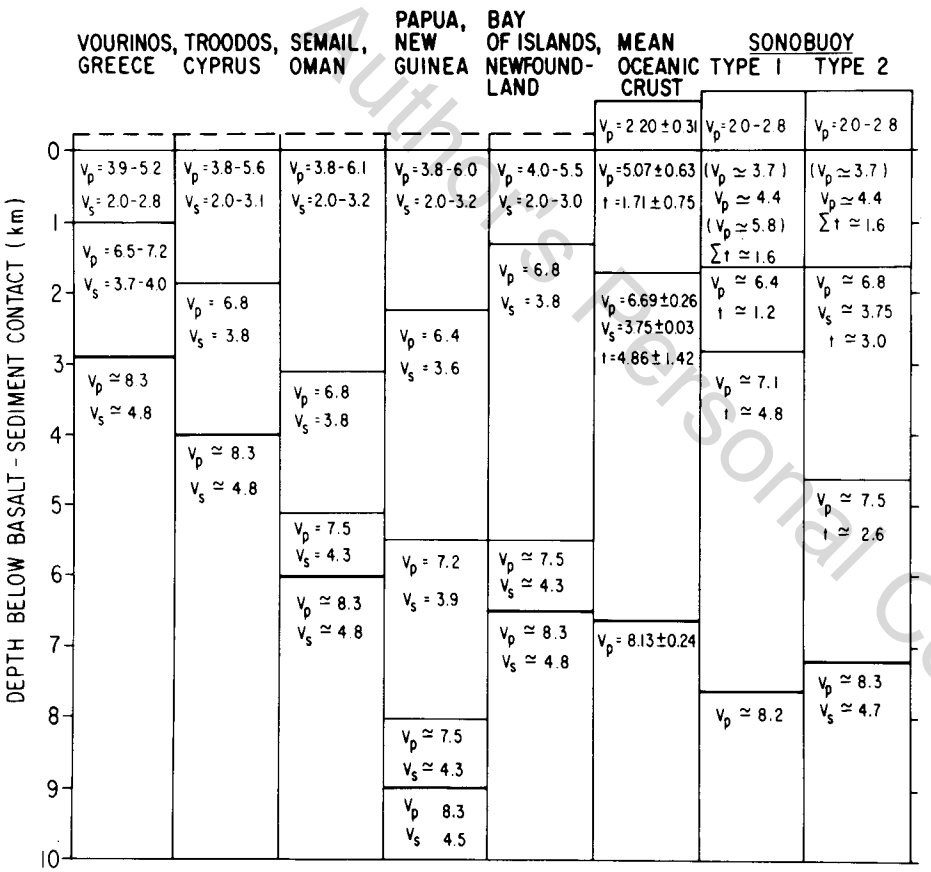

Fig. 7. Seismic layering of major ophiolites compared with ocean crustal structure.

Author's Personal Copy

related to high shear velocities. Because the late differentiates occur as dikes, sills and pods, the velocity inversions are likely to be laterally discontinuous.

The various seismic layers, their approximate velocities and thicknesses are summarized in Fig. 7 for the five major ophiolite complexes along with the three layer mean oceanic crust of Raitt (1963) and two crustal models from sonobuoy data (Christensen and Salisbury, 1975). Low velocity zones have been excluded because they are largely undetected in refraction seismology and sonobuoy studies. Since relatively small velocity increases are asssociated with the 7.5 km/sec layers of the Semail, Papua and Bay of Islands massifs, these layers would also likely be undetected in normal refraction surveys and their thicknesses would be included with the overlying units. Sonobuoy studies, on the other hand, would likely detect the 7.5 km/sec layers.

In addition to using simple crustal averages, it is also instructive to compare the velocity structures of the ophiolites with those of refraction seismology by plotting velocities versus layer thicknesses. In Fig. 8A, observed

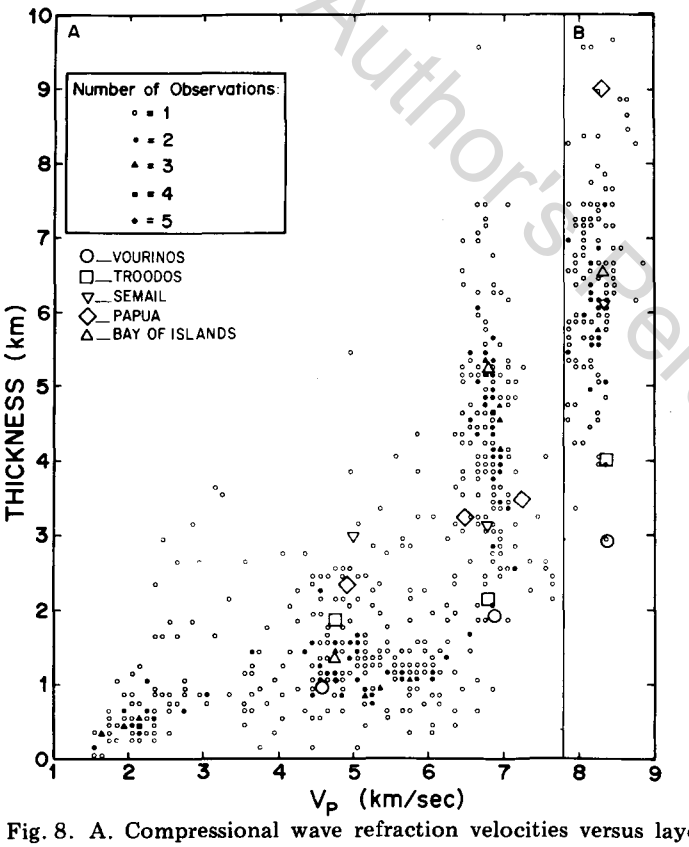

Fig. 8. A. Compressional wave refraction velocities versus layer thicknesses. B. Mantle compressional wave velocity versus cumulative crustal thickness compared with ophiolite seismic layering.

Author's Personal Copy

velocities from 415 main ocean basin sites (Christensen and Salisbury, 1975) are plotted against their associated layer thicknesses and in Fig. 8B mantle velocities are plotted against the thicknesses of the overlying crustal sections. Superimposed on this figure are the velocities and layer thicknesses for the ophiolites, which would be observed from seismic refraction studies. Comparisons of this type leave no doubt that there are striking similarities between ophiolite seismic structures and oceanic crustal seismic structures.

ACKNOWLEDGEMENTS

I am indebted to M.H. Salisbury for many stimulating discussions and help which contributed to this paper. D. Borns assisted in the petrography. L. Goullaud provided several samples from the Trinity Complex. Financial support was provided by the Office of Naval Research contract N—00014—75—C—0502.

REFERENCES

Avé Lallemant, H.G., 1976. Structure of the Canyon Mountain (Oregon) ophiolite complex and its implication for seafloor spreading. Geol. Soc. Am., Spec. Pap., 173: 1—49.

Bailey, E.H., Blake, M.C., Jr. and Jones, D.L., 1970. Onland Mesozoic oceanic crust in California coast ranges. U.S. Geol. Surv., Prof. Pap., 700—C: C70—C81.

Barrett, D.L. and Aumento, F., 1970. The mid-Atlantic ridge near 45°N, 11, seismic velocity, density and layering of the crust. Can. J. Earth Sci., 70: 1117—1124.

Birch, F., 1960. The velocity of compressional waves in rocks to 10 kilobars, 1. J. Geophys. Res., 65: 1083—1102.

Birch, F., 1961. The velocity of compressional waves in rocks to 10 kilobars, 2. J. Geophys. Res., 66: 2199—2224.

Brothers, R.N., 1959. Flow orientations of olivine. Am. J. Sci., 257: 574—584.

Christensen, N.I., 1965. Compressional wave velocities in metamorphic rocks at pressures to 10 kbar. J. Geophys. Res., 70: 6147—6164.

Christensen, N.I., 1966a. Elasticity of ultrabasic rocks. J. Geophys. Res., 71: 5921—5931.

Christensen, N.I., 1966b. Shear wave velocities in metamorphic rocks at pressures to 10 kbar. J. Geophys. Res., 71: 3549—3556.

Christensen, N.I., 1970. Possible greenschist facies metamorphism of the oceanic crust. Geol. Soc. Am. Bull., 81: 905—908.

Christensen, N.I., 1972. The abundance of serpentinites in the oceanic crust. J. Geol., 80: 709—719.

Christensen, N.I. and Salisbury, M.H., 1972. Sea floor spreading, progressive alteration of layer 2 basalts, and associated changes in seismic velocities. Earth Planet. Sci. Lett., 15: 367—375.

Christensen, N.I. and Salisbury, M.H., 1975. Structure and constitution of the lower ocean crust. Rev. Geophys. Space Phys., 13: 57—86.

Christensen, N.I. and Shaw, G.H., 1970. Elasticity of mafic rocks from the mid-Atlantic ridge. Geophys. J., 20: 271—284.

Coleman, R.G. and Peterman, Z.E., 1975. Oceanic plagiogranite. J. Geophys. Res., 80: 1099—1108.

Davies, H.L., 1971. Periotite-gabbro-basalt complex in eastern Papua: an overthrust plate of oceanic mantle and crust. Bull. Bur. Miner. Res. Geol. Geophys. Aust., 128: 1—47.

Author's Personal Copy

Fox, P.J., Schreiber, E. and Peterson, J.J., 1973. The geology of the oceanic crust: compressional wave velocities of oceanic rocks. J. Geophys. Res., 78: 5155—5172.

Goullaud, L., 1975. Structure and petrology in the Trinity mafic-ultramafic complex, Klamath Mountains, Northern California. Geol. Soc. Am., Abstr. Progr., 7: 321.

Hamilton, E.L., Moore, D.G., Buffington, E.C., Sherrer, P.L. and Curray, J.R., 1974. Sediment velocities from sonobuoys: Bay of Bengal, Bering Sea. Japan Sea, and North Pacific. J. Geophys. Res., 79: 2653—2668.

Hyndman, R.D. and Drury, M.J., 1976. The physical properties of oceanic basement rocks from deep sea drilling on the Mid-Atlantic ridge. J. Geophys. Res., 81: 4042—4059.

Kroenke, L.W., Manghnani, M.H., Rai, C.S., Fryer, P. and Ramananantoandro, R., 1976. Elastic properties of selected ophiolite rocks from Papua, New Guinea: nature and composition of oceanic lower crust and upper mantle. In: G.H. Sutton, M.H. Manghnani and R. Moberly (Editors), The Geophysics of the Pacific Ocean Basin and Its Margin. Woollard Volume — Geophys. Monogr., Am. Geophys. Union, 19: 407—421.

Lipman, P.W., 1964. Structure and origin of an ultramafic pluton in the Klamath Mountains, California. Am. J. Sci., 262: 199—221.

Manghnani, M.H. and Woollard, G.P., 1968. Elastic wave velocities in Hawaiian rocks at pressures to ten kilobars. In: L. Knopoff, C.L. Drake and P.J. Hart (Editors), The Crust and Upper Mantle of the Pacific Area. Geophys. Monogr., Am. Geophys. Union, 12: 501—516.

Moores, E.M., 1969. Petrology and structure of the Vourinos ophiolitic complex of northern Greece. Geol. Soc. Am., Spec. Pap., 118: 1—74.

Nur, A. and Simmons, G., 1969. The effect of saturation on velocity in low porosity rocks. Earth Planet. Sci. Lett., 7: 183—193.

Page, B.M., 1972. Oceanic crust and mantle fragment in subduction complex near San Luis Obispo, California. Geol. Soc. Am. Bull., 83: 957—972.

Peterson, J.J., Fox, P.J. and Schreiber, E., 1974. Newfoundland ophiolites and the geology of the oceanic layer. Nature, 247: 194—196.

Poster, C.K., 1973. Ultrasonic velocities in rocks from the Troodos massif, Cyprus. Nature, 243: 2—3.

Raitt, R.W., 1963. The crustal rocks. M.N. Hill (Editor), The Sea, Vol. 3. Wiley, New York (N.Y.), pp. 85—102.

Reinhardt, B.M., 1969. On the genesis and emplacement of ophiolites in the Oman Mountains geosyncline. Schweiz. Mineral. Petrogr. Mitt., 49: 1—30.

Simmons, G., 1964. The velocity of shear waves in rocks to 10 kbar, 1. J. Geophys. Res., 69: 1123—1130.

Smith, C.H., 1958. Bay of Islands igneous complex, western Newfoundland. Geol. Surv. Can., Mem. 290: 1—132.

Thayer, T.P., 1963. The Canyon Mountain complex, Oregon, and the Alpine mafic magma stem. U.S. Geol. Surv., Prof. Pap., 475 C: C82—C85.

Williams, H., 1971. Mafic-ultramafic complexes in western Newfoundland Appalachians and the evidence for transportation: a review and interim report. Proc. Geol. Assoc. Can., 24: 9—25.

Wilson, R.A.M., 1959. The geology of the Xeros—Troodos area. Cyprus, Geol. Surv. Dep., Mem., 1: 1—184.

Author's Personal Copy